Gas enclosure in ice: age difference and fractionation

Thomas Blunier† and Jakob Schwander

Climate and Environmental Physics, Physics Institute, University of Bern, Sidlerstrasse 5, CH-3012 Bern, SWITZERLAND
†now at Geosciences, Princeton University, Guyot Hall, Princeton, New Jersey 08544, USA

Abstract: Ice from polar ice sheets and from glaciers bear a unique archive of the past atmospheric composition. However, the air extracted from the ice gives not only information about the atmospheric composition. Through the complex manner of gas occlusion the extracted gases can also provide information about physical properties at the drill site in the past.

Since air in the porous firn layer on the surface of the ice sheet exchanges with the overlying atmosphere it has a mean age which is younger than the age of the surrounding ice when it gets enclosed in bubbles at 50–150 m below the surface. The difference between the age of the ice and the mean age of the gas at close-off depth has been calculated using a dynamic model for firn densification and diffusional mixing of the air in the firn including the heat transport in the firn and temperature dependence of the close-off density. The gravitational fractionation of $\delta^{15}N$ which is constant in the atmosphere gives an independent measure of the close-off depth. These results are generally in agreement with the modelled close-off depth.

The occlusion process adds new information to the gas record. Since the occlusion process is temperature sensitive the depth difference between corresponding events in the ice and in the gas record allows in principle to reconstruct the temperature history.

Temperature reconstructions for Greenland based on borehole temperature measurements suggest that the temperature calculated based on the spatial $\delta^{18}O$/temperature relation does at least not hold for the glacial/interglacial temperature increase. Under the assumption that the $\delta^{18}O$ and the CH_4 signal in the GRIP and GISP2 ice core are synchronous, justified by the close resemblance of the two records, they corroborate that the changed $\delta^{18}O$/temperature relation is also valid for short term variations like Dansgaard-Oeschger events.

Recently a new aspect of the $\delta^{15}N$ record has been brought up. During fast temperature changes the $\delta^{15}N$ concentration in the firn changes due to thermal diffusion. This effect can be used to determine independently temperature changes during fast climatic events.

Physics of Ice Core Records
Edited by T. Hondoh
Hokkaido University Press, 2000, Sapporo

1. Introduction

The paleo-archive of glaciers and ice sheets is unique as it is the only one which records also directly the atmospheric composition. Samples of atmospheric air are found in the bubbles of the ice. However, the archive samples not like a flask sample. The upper 50–150 m of an ice sheet are open porous, this section is called firn and it is but at the bottom of that zone where the gas is occluded in the ice. Therefore atmospheric air exchanges with the air in the firn. As a consequence 1) the concentration of a gas species in the firn changes relative to its atmospheric concentration due to physical and in case of reactive gases chemical processes. 2) the age of the gas in an occluded air bubble is less than the age of the surrounding ice. This age difference (Δage hereafter) is temperature and accumulation dependent.

Not all glaciers and ice sheets are equally useful regarding the past atmospheric composition. We distinguish three types of glaciers: 1) cold glaciers where the temperature is always below the melting point and where snow falls as dry snow. 2) cold glaciers where surface melting occurs and meltwater percolates into the firn. 3) temperate glaciers which are except for the surface snow at the pressure melting point and where a network of water carrying capillary veins exists between the ice grain. Where melting occurs gas content and gas composition may be altered by chemical reactions taking place in aquatic systems or by physical gas exchange between the gaseous and the aquatic sections. We look at cold glaciers of type 1 where such reactions are excluded. However, such glaciers are difficult to find. Also in Central Greenland where the present annual mean temperature is below −30 °C sporadic surface melting occurs. However, when the occurrence of melt layers is small it may be regarded as a type 1 glacier. In the first part we are discussing the processes taking place in the firn in general. Then we will on the example of Central Greenland discuss the occlusion and the resulting Δage under present day conditions. Further we will calculate Δage for past times also in view of the temperature information stored in it.

2. Firn transformation

The density of the firn at the surface is around 350 kg/m^3 corresponding to a porosity of about 0.6–0.7. Higher surface densities may result when the firn is compacted by wind. Martinerie et al., found densities in the range of 330–490 kg/m^3 with a strong dependence on wind speed especially above 6 m/s.

The firn is compacted by the weight of the overlaying layers and as a result of water vapour diffusion. Between the surface and a density of about 550 kg/m^3 the firn metamorphoses is dominated by the rearrangement of the firn grains in order to get to a closer packing. Further down the rearrangement of the grains leads to no significant density increase. There sintering and plastic deformation become the most important processes. The border of the two zones clearly manifests in the density versus depth profile. Around a density of 800 kg/m^3 the pores are gradually pinched off and form bubbles in the ice. This zone is called firn-ice transition [1] and spans about the lowest 10 % of the total firn column of between 50 and 150 m. Under cold conditions the major part of the gas (~90 %) is

occluded within the firn-ice transition and almost no gas is closed off above the depth where a density of 790 kg/m^3 is reached.

The density versus depth increase was described by Herron and Langway based on an empirical study of Greenland and Antarctic sites in the temperature range of −15 to −57 °C [2]. Due to the different main densification processes above and below 550 kg/m^3 the densification is described differently for the section above and below this critical density. Another approach for the density of the firn layer was built by Pimienta and Barnola [3]. For densities exceeding 550 kg/m^3 they describe the densification process in a more physical way but still based on empirical data. In Figure 1 the calculated firn density from the two models is compared to the measured densities for Central Greenland [4]. The two models compare well to the data and between each other. The uncertainty of the input parameters accumulation and temperature is larger than the uncertainty of the models. Depending on the site (especially temperature and accumulation) the age of ice in the close-off region is up to 3000 yr old under present day conditions and was significantly larger during periods of colder climate with reduced accumulation and temperature.

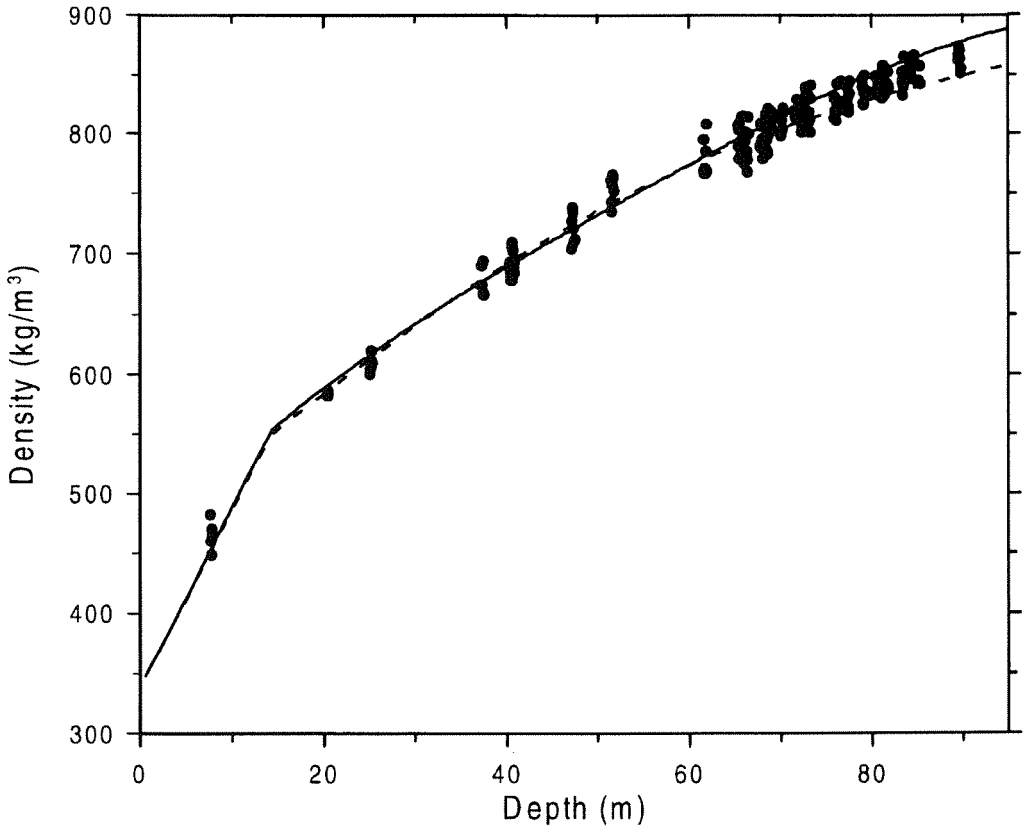

Figure 1: Density (dots) versus depth at Summit, Central Greenland [4]. The lines through the density data are calculated with the Herron-Langway [2] (dotted line) and the Pimienta-Barnola model [3] (solid line).

3. Processes changing the air composition in the firn

Regarding processes affecting the air composition in the firn, the firn layer may be divided into three zones. The division into these zones is suggested by the succession of the $\delta^{15}N$ concentration in the firn [5] (Figure 2). $\delta^{15}N$ is constant in the atmosphere over time. Therefore any change in the $\delta^{15}N$ composition in the firn must be attributed to physical processes in the firn. Under constant climatic conditions the $\delta^{15}N$ concentration is unchanged over the first few meters of the firn. In the second zone it gradually increases to reach again a constant value in the third zone. The uppermost zone, called convection zone, is permanently exchanging air with the atmosphere by convection and has therefore atmospheric concentration. This zone may be more or less thick depending on local characteristics. Below in the static-air column gases exchange mainly by molecular diffusion. The bottom section is the non diffusive zone. There gas is no longer exchanging with the overlaying layers although it is not yet completely isolated.

In a static-air column an equilibrium between molecular diffusion and gravitational settling is reached for each gas component according to the barometric formula [6, 7]. As a consequence two gas

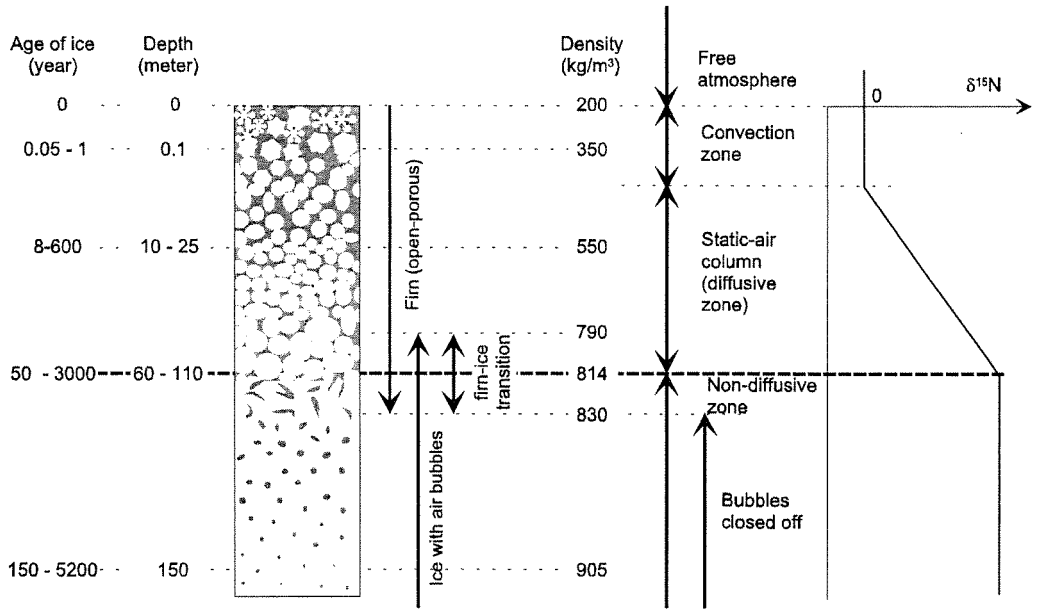

Figure 2: Sketch of the firn column. The indicated depths and age ranges are typical for polar ice sheets and do not necessarily apply for mountain sites. Air bubbles mainly form at densities between 790 and 830 kg/m^3. Subdivision into zones suggested by Sowers et al. [5] and the corresponding $\delta^{15}N$ profile are given on the right side. Convection in the uppermost layer results in a $\delta^{15}N$ plateau. In a molecular-diffusive regime the $\delta^{15}N$ increases linearly with depth due to gravitation. Diffusion is expected to stop somewhat above the final close-off of air bubbles. Under stationary conditions $\delta^{15}N$ remains constant in this non-diffusive zone.

components with a molecular mass difference of ΔM_{ij} experience a fractionation δ_{ij} from their initial relationship which is increasing with depth (equation 1).

$$\delta_{ij}(z) = \left[e^{\left(\frac{\Delta M_{ij} g z}{RT} \right)} - 1 \right] \cdot 1000‰ \cong \frac{gz}{RT} \Delta M_{ij} \cdot 1000‰ \quad (1)$$

where: z = depth (m); ΔM_{ij} = difference of molecular weight of two gases (kg/mol); g = acceleration due to gravity (m/s^2); R = gas constant (= 8.314 J/(K·mol)); T = temperature (K).

This allows to calculate the height of the static air column from the fractionation of two gas components with a constant relationship in the atmosphere as for instance the isotopes of nitrogen or argon. As the firn flows to deeper depth also the air in it does and the reached equilibrium will not be complete. However, the age of the ice at the firn-ice transition is generally large compared to the diffusive mixing time of the air in the firn and we must correct for an incomplete equilibrium only at very high accumulation sites. For the low accumulation site Vostok (Antarctica) the measured $\delta^{15}N$ firn concentrations fit well to the predicted slope of 0.542 ‰/100 m, according to the gravitational settling at –55.5 °C [8].

The $\delta^{15}N$ increase with depth lets us calculate the diffusive column height but it gives us no information about the height of the convection or the non diffusive zone. The difference between the diffusive column height and the close-off depth reaches from 5 to 34 m under present day conditions (here close-off depth is the mean pressure isolation depth after Martinerie et al. [9]). No correlation between this difference and site parameters was found so far [5]. Thus $\delta^{15}N$ can only be used for an estimate of the close-off depth. However, generally diffusive column height from $\delta^{15}N$ values are in agreement with close-off depth, meaning that diffusive column heights are lower than close-off depths.

Besides molecular diffusion other processes are affecting the firn air, whose importance vary from site to site depending on: Surface topography, wind speed, wind direction distribution, permeability (icy layers), temperature, pressure, accumulation rate. We can distinguish processes leading to advection and diffusion processes.

3.1 Transport of air masses

Various processes can lead to the transport of air masses in the firn. Atmospheric pressure variations make the firn 'breathe'. The displacement of the firn air at a certain depth is proportional to the total air volume between this depth and the firn-ice transition, and inversely proportional to the open porosity. Wind over an uneven surface leads to local pressure differences inducing air flow along pressure gradients. Depending on the size of the surface undulations the induced flow penetrates more or less deeply into the firn [10]. However, no correlation between the thickness of such a layer and wind speed has been found so far [5].

Wind pumping could induce temperature gradients and thereby density gradients that might eventually cause small convection flows which could maintain themselves even after the wind has calmed down. Free convection has so far only been observed in shallow snow covers [11] and it is not known whether such convection cells

also occur in glacier firn.

During summer the stratification of the air in the firn pores is stable, whereas in winter cold air at the snow surface tends to sink into the firn. Finally air is forced to flow through the firn pores by the densification process itself. As the pore volume decreases with depth air is squeezed out and moves upwards relative to the ice matrix. The corresponding air flow speeds are largest near the surface where they are of the order of the snow accumulation rate. Local high air flows can however also occur at the firn-ice transition or in melt layers when the permeable fraction of a dense, partly impermeable layer becomes very small. Air from less dense layers underneath is then squeezed through the few permeable 'holes' in the dense layer.

All mixing processes are strongly influenced by the presence or absence of icy layers resulting from surface melting during summer. Surface melting is rare if the mean annual temperature is below –30 °C. If icy layers exist the geometry of air flow paths is highly complex, and, to our knowledge, no quantitative investigations exist for this case.

3.2 Diffusion processes

The most important diffusion process is definitely molecular diffusion. Molecular diffusion may be driven by a concentration gradient, gravitation or also by a temperature gradient. Under constant climatic conditions the $\delta^{15}N$ concentration reaches an equilibrium between gravitation and concentration driven diffusion in the static air column; neglecting the upward flow of air resulting from the densification itself. When the temperature is changing thermal diffusion in the firn gets important. When a gas mixture is exposed to a temperature gradient it will unmix by thermal diffusion and the heavier gas will tend to the colder end. This effect is known since the 1940s but only recently Severinghaus et al. [12] have used it in the field of ice core research.

In a constant temperature gradient, a steady state is reached in which thermal diffusion is balanced by diffusion along the resulting concentration gradient. The difference in the isotope ratios R and R_0 at temperatures T and T_0 calculates by:

$$\delta = \left[\frac{R}{R_0} - 1\right] \cdot 1000 = \left[\frac{T}{T_0} - 1\right]^{\alpha} \cdot 1000 \qquad (2)$$

During rapid climate change thermal gradients appear and persist for several hundred years in the firn column due to the low heat diffusion. During temperature rise heavier isotopes will flow to the deeper colder end while during climate cooling the heavier isotopes will flow to the surface. The speed of the thermal diffusion is that of ordinary (molecular) diffusion [8]. Therefore the signal from thermal diffusion will reach the bottom of the firn column long before the temperature equilibrates and will be recorded there. The gas composition will closely approach a steady state with respect to the firn temperature such that equation 2 should be valid [12]. This has been shown by a model study by Severinghaus et al. [12]. Therefore temperature changes can be derived directly from the deviation of an isotopic ratio from its steady state equilibrium given by equation 2.

Diffusion pumping, transport of a gas species by the diffusion movement of a 'carrier' component, has not been observed in ice cores so far. However, the effect has been observed in dunes [13] and in

experimental setups where strong fluxes of water vapour occur.

3.3 Δage and age distribution

A consequence of the gas exchange between the atmosphere and the firn is that the age of the air in the pore space and in the bubbles of the ice below the firn-ice transition is younger than the surrounding ice. The age distribution of the air components in the bubbles of the ice is controlled by two processes: 1) the air mixing in the firn leads to a characteristic distribution of the age of gas molecules as a function of depth (the age of a gas molecule is defined as the time elapsed since it has for the last time crossed the atmosphere-snow boundary), 2) as important for the width of the total age distribution is that the formation of isolated air bubbles or clusters occurs gradually over a depth range of typically 10 m, i.e. at a certain depth in the ice we have a bubble population of which the individuals had been formed at different times. Thus there is a second convolution of the age distribution after the firn air mixing process. However approaching the close-off region diffusivities get very low and reach zero before the major part of the bubbles are formed. How much the gradual close-off increases the width of the age distribution depends mainly on the time the ice needs to cross the bubble close-off zone, which is about inversely proportional to the accumulation rate.

4. Diffusion model

Schwander et al. [4] have set up a one dimensional diffusion model which allows calculation of the concentration of a gas species versus depth starting from its atmospheric concentration history. The model is based on pure molecular diffusion and includes gravity [6, 7]. This leads to an increase in the heavier components versus depth. Additional mixing due to convection or ventilation is not included in the model. Yet, it takes into account the upward flow of air due to the densification of the firn. For radioactive components the decay is included in the model.

Diffusion coefficients for trace gases in firn are fundamental for the firn diffusion model. So far diffusion coefficients have only been measured directly at Siple Station, Antarctica, by Schwander et al. [14]. The site has a mean annual temperature of –24 °C and an accumulation rate of 0.5 m water equivalent per year. Diffusion coefficients for CO_2 and O_2 have been measured by measuring the broadening of a gas packet in a carrier gas (N_2). As expected the diffusivity decreases with porosity (Figure 3) but reaches zero already before the open porosity disappears; well above the end of the bubble formation zone. This implies that only the fraction of bubbles formed at depth above this density level adds additional broadening to the age distribution. Since this portion is small it may be neglected regarding the age distribution for sites comparable to Siple Station. On Siple Station Schwander [6] found the following empirical dependencies [6].

$$\text{closed porosity } s_{cl} = \begin{cases} s \cdot e^{75\left[\frac{\varrho}{830}-1\right]} & \text{for } 0 < \varrho < 830\,\text{kg/m}^3 \\ s & \text{for } \varrho > 830\,\text{kg/m}^3 \end{cases}$$

$$\text{diffusivity } D = D_0\left(1.7 s_{op} - 0.2\right) \qquad (3)$$

where s is the total porosity ($s = 1 - \rho/\rho_i$; ρ_i is the pure ice density) and s_{cl} the closed porosity. The open porosity s_{op} is by

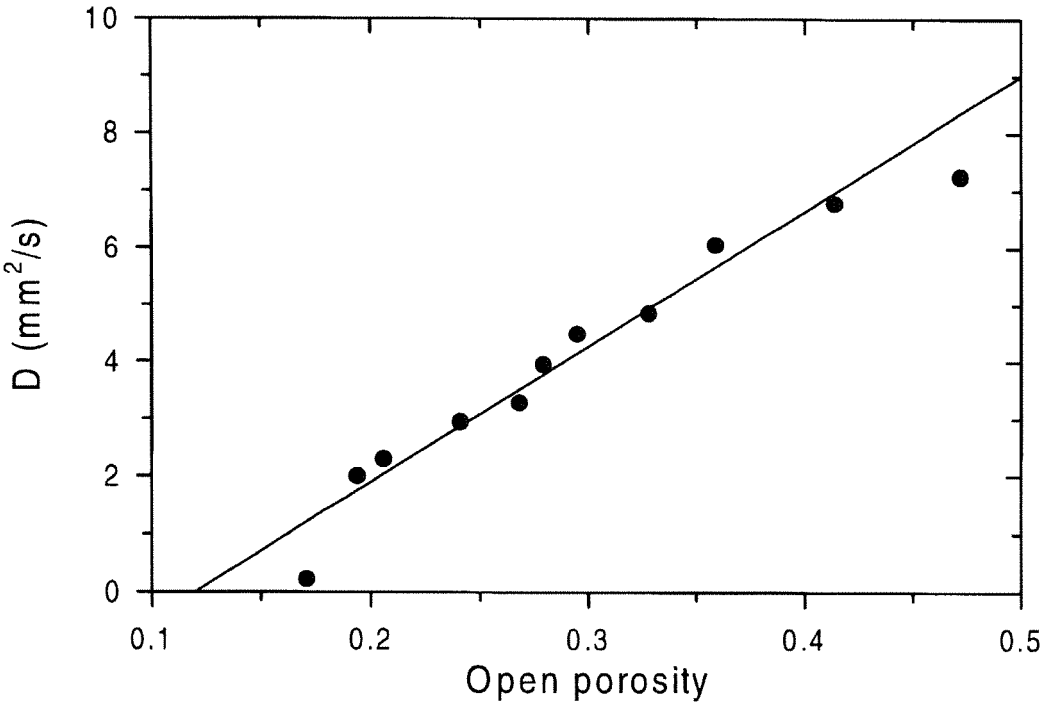

Figure 3: Diffusion coefficient versus open porosity from Siple Station [14].

definition: $s_{op} = s - s_{cl}$. D_0 is the diffusion coefficient of the considered gas in air.

5. Results from Central Greenland

The firn air has been investigated in detail at Summit, Central Greenland (72.58°N, 37.64°W) in the frame of the Eurocore drilling project [4]. This project is the predecessor of the better known GReenland Ice core Project (GRIP) carried out at the same location. Results from the firn air study apply directly to the GRIP core.

5.1 Present Δage

Diffusion coefficients have not been measured at Central Greenland. Therefore the question arises whether or not it is justified to use the diffusion coefficients found for Siple Station. The closed porosity versus density function has been compared to the Siple Station data and was found to be similar; thus also the open porosity is similar. The two sites are both polar sites and are dominated by the dry sintering process thus we may expect that also the tortuosity is similar. We assume that Siple Station diffusivities are valid for other sites observing comparable site conditions when the diffusivities are adjusted for temperature and pressure as well as for the gas species.

In Figure 4 modelled and measured firn concentrations for ^{85}Kr, CO_2 and CH_4 are compared. All trace gases decrease with depth as a consequence of the ongoing atmospheric concentration increase [4]. The decreasing trend also reveals that the

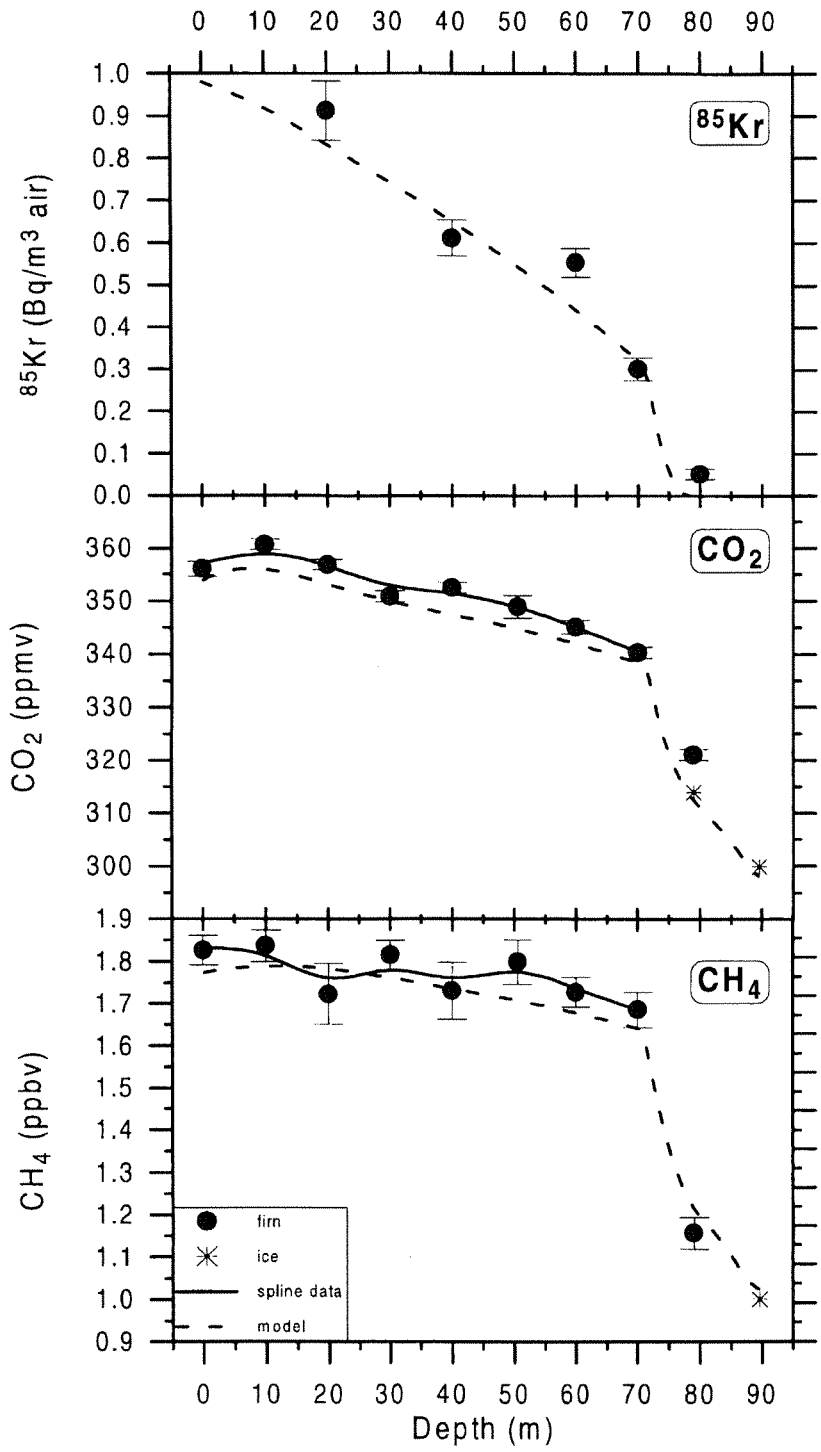

Figure 4: ^{85}Kr, CO_2 and CH_4 concentrations in firn and ice from Summit Central Greenland together with modelled firn concentrations bases on the atmospheric concentration history [4].

ventilation time in the firn is considerable. Below the close-off depth the concentrations decrease with depth reflecting the atmospheric increase modulated by the speed of the downward ice flow. According to the measured data the close-off depth is found in about 70 m. The concentrations of ^{85}Kr, CO_2 and CH_4 at that depth correspond to atmospheric concentrations 10–12 yr ago.

The input data for the model was obtained adjusting data from the world-wide concentration evolution to data from nearby measurement stations [4]. The modelled concentrations fit generally well the measured firn concentrations. The half-life of only 10.8 yr and the rapid atmospheric increase make ^{85}Kr an excellent tracer to investigate firn ventilation. In two points the ^{85}Kr data are more than three standard deviations higher than the modelled concentrations. These values most probably reflect contamination in the laboratory either with traces of fresh air or a substance interfering with the β-energy spectrum of ^{85}Kr. The good agreement between the measured and the modelled firn concentrations confirms that molecular diffusion is the dominant process in the firn. The slope of the modelled data changes abruptly at about 71 m. Below that depth the diffusion coefficient is zero according to the density-diffusivity ratio. The good agreement between the model and the data at 79 and 89.6 m shows that the exchange with overlying layers is essentially stopped below 71 m. Although the model includes no convection zone it reproduces nicely the measured firn concentrations. This does not prove that there is no convective zone at Summit since the diffusivity in the upper 20 m of the firn itself is so effective that it almost catches up with a convective mixing. However, the generally good agreement between the ^{85}Kr data and the model suggests a convection zone of significantly less than 20 m. The age of the ice at the upper border of the non diffusive zone is 220 yr. The mean age of the air is about 10 yr and Δage calculates to 210 yr.

At Summit the gas occlusion takes mainly place below 71 m that is already in the non diffusive zone and only 20 % of the gas is occluded in the diffusive zone. The age distribution at close-off is thus mainly determined by the diffusion process in the firn and not by the gradual occlusion. In Figure 5 the modelled age distribution for CO_2 is shown. The standard deviation of the age distribution at close-off is 7.5 yr.

5.2 Δage under changing climatic conditions

The difference between the age of the ice and the age of the air under different climatic conditions can be assessed by the determination of the depth of the firn-ice transition and the age of the ice at this depth using a firn densification model on one hand and the calculation of the age of the air at the transition depth with a diffusion model on the other hand. For the present situation at Summit both the empirical densification model by Herron-Langway (H-L) [2] and the semi empirical model by Pimienta-Barnola (P-B) [3, 15] compare well to the measured densities (Figure 1). In order to calculate densification over climatic changes the steady state densification model from H-L has to be brought into a dynamical version [16]. Down to a density of 550 kg/m^3, the P-B makes use of the H-L model. Here the P-B approach was used [16] with one important extension. Since the model is used for the study of rapid climate change the firn

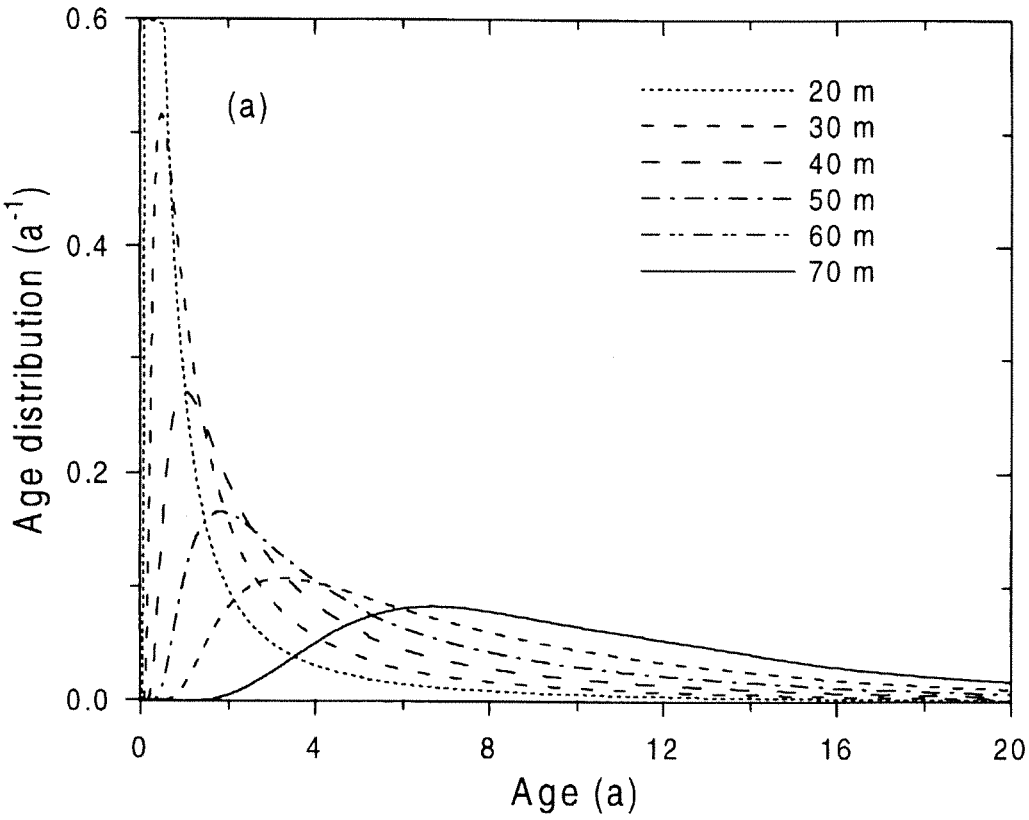

Figure 5: Age distribution for CO_2 in the firn of Summit, Central Greenland calculated with the diffusion model [4].

temperature versus depth is not constant in time which affects the densification process. Therefore the heat transfer in the firn was added to the model by Schwander et al.[16].

In order to calculate the age of the ice at the bubble close-off depth the close-off density under past climatic conditions has to be known. Based on total gas content measurements from Martinerie et al. [17] (Figure 6) the relation between close-off density and temperature can be described with the following equation:

$$1/\rho_{co}(\mathrm{m^3/kg}) = 1/\rho_{ice} + 6.95\times10^{-7}(T+273.16) - 4.3\times10^{-5} \quad (4)$$

where ρ_{ice} is the pure ice density (in kg/m^3) and T is the mean annual temperature (in °C) at the site. The so determined close-off density is the average density at which bubbles are isolated from the atmosphere. However this density is not identical to the density where air exchange stops. From the present day study at Summit the air isolation depth is 71 m corresponding to a density of only 814 kg/m^3 [4] compared to a close-off density of 828 kg/m^3 from total gas measurements [18]. This difference is due to the presence of a non diffusive zone. Assuming that the size of the non-diffusive zone has not significantly changed in time 14 kg/m^3 was subtracted from equation 4 for the Δage calculation. Hereafter close-off depth (COD) refers to the depth where this

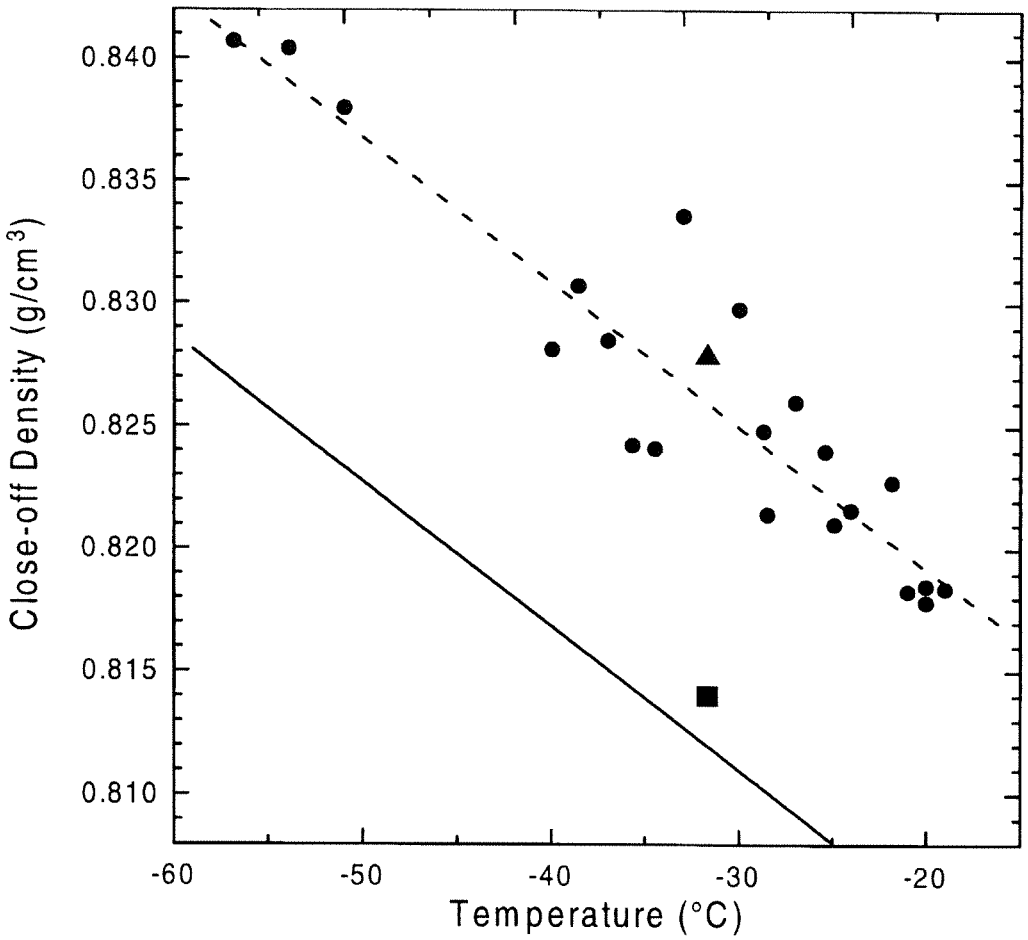

Figure 6: Close-off density versus temperature. Dots are from total gas measurements [9, 17]. The triangle is the Summit close-off density from total gas measurements [18]. The filled square is the density of the firn isolation depth from the diffusion study at summit [4]. For the calculation of Δage over time the relation from total gas measurements (dotted line, equation 4) was lowered by 14 g/cm^3 in accordance to the GRIP results (solid line).

reduced density is reached.

The age of the air is relatively small compared to the age of the ice. Under present day conditions it is less than 5 % of the Δage and its portion is decreasing for colder climate. Therefore the age of the air was parametrized according to the Summit results [16].

$$\text{gasage(year)} = 10 \cdot (\text{COD}/70)^2 \cdot \left(\frac{241.45}{T}\right)^{1.85} \quad (5)$$

where COD is the close-off depth calculated by the densification model in meter and T is the temperature in K. This approach assumes that the diffusive equilibration time is proportional to the square of the firn thickness and that D is proportional to $T^{1.85}$ [19]. Δage can now be calculated as the difference from the age of the ice deduced from the densification model and the age of the air approximated by equation 5.

Data used to determine the parameters of the densification model stem from sites in Greenland and Antarctica where the densification process is dominated by dry sintering. They cover an annual mean temperature range from –15 to –57 °C and mean accumulations from 0.02 to 0.5 m water equivalent based on present day conditions at various sites. The date used to obtain the close-off density covers the temperature range from –19 to –57 °C. This range includes all present and past temperature and accumulation rates for the Summit location over the last 100 kyr. For densities above 550 kg/m^3 the densification model is based on physical processes where the parameters have been determined empirically. We do not expect that the physics of the densification has changed over time. The error for the calculation of the age of the air at close-off can be neglected since it is more than 10 fold lower than the age of the ice at close-off. Therefore the Δage model is valid for the

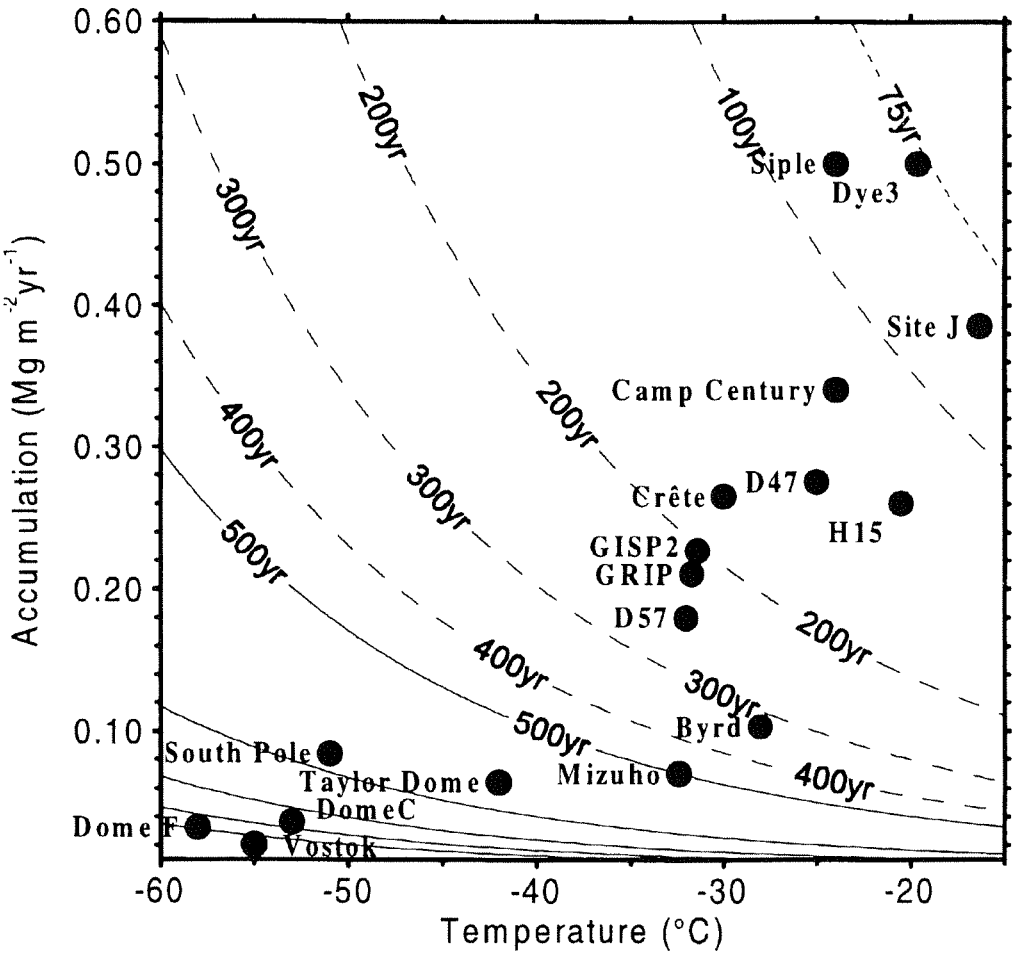

Figure 7: Age difference between the ice and the air of the bubbles as a function of temperature and accumulation rate calculated with the Schwander model [16] for stationary conditions. Present day conditions of temperature and accumulation for various polar sites are indicated. (Solid lines denote a contour level distance of 500yr.)

entire Greenland record under the assumption that the densification process was constant in time. In Figure 7 variations of Δage depending on accumulation and temperature are plotted together with the parameters for several drilling sites under present day condition.

6. Temperature estimates for Central Greenland

The Δage model relates accumulation and temperature to Δage and COD. For Greenland and Antarctica several temperature estimates for the past are under debate. With independent estimates of Δage or COD, it is possible to judge over these temperature scenarios by comparison to the modelled Δage or COD. Such a study has been done by Schwander et al. [16] for Central Greenland.

Past Greenland surface temperatures can be estimated from today's spatial relationship between mean annual surface temperature and the mean $\delta^{18}O$ of the precipitation (hereafter referred to as $\delta^{18}O$) [20, 21]. The data were described with the following equation:

$$\delta^{18}O(‰) = 0.67T - 13.7 \qquad (6)$$

where T is the temperature in °C. The slope of this function, $d(\delta^{18}O)/dT$ (referred to as $\alpha_{spatial}$) is the product of various equilibrium and kinetic isotope effects associated with evaporation and condensation of water as it travels from its source to the final precipitation site today [21]. On the other hand high-precision borehole temperature measurements [22, 23] suggest that the long term $d(\delta^{18}O)/dT$ coefficient ($\alpha_{temporal}$) was probably closer to 0.33, doubling the estimate for the temperature difference from the last glacial to the Holocene from today's relation. Unfortunately, the borehole inversion techniques cannot resolve the magnitude of the fast temperature variations of the stadial/interstadial events during the last glaciation and it is possible that the "true α" has varied with time.

For the two extreme temperature estimates [21–23] ($\alpha_{spatial}$ and $\alpha_{temporal}$) and accumulations derived from measured annual layer thickness in combination with ice flow modelling Δage and COD estimates were computed for the GRIP and the GISP2 (28km to the west of GRIP) site over the last 100 kyr. In Figure 8 the results for the last 50 kyr are shown for the GRIP ice core, the results for the GISP2 core are comparable to the GRIP results. (The total results from the GRIP and the GISP2 core can be found in the original publication by Schwander et al. [16].) For the lower temperature scenario ($\alpha_{temporal}$) calculations have been made with and without heat diffusion in the firn. Including heat diffusion weakens the immediate response of Δage and COD to a temperature change and leads therefore to a smoother Δage and COD function. Excluding the heat diffusion in the firn leads to deviations of over 200 yr and 20 m for Δage and COD, respectively. The difference of Δage and COD between the two temperature scenarios reaches up to 400 yr and 50 m for the GRIP location respectively. These differences are large; thus if it is possible to get independent estimates for either of the two parameters the model allows to decide which temperature scenario is the more likely one.

An independent Δage estimate can be obtained whenever a climatic event manifests simultaneously in the ice and in the gas record by counting the annual layers between the ice and the gas event. The CH_4

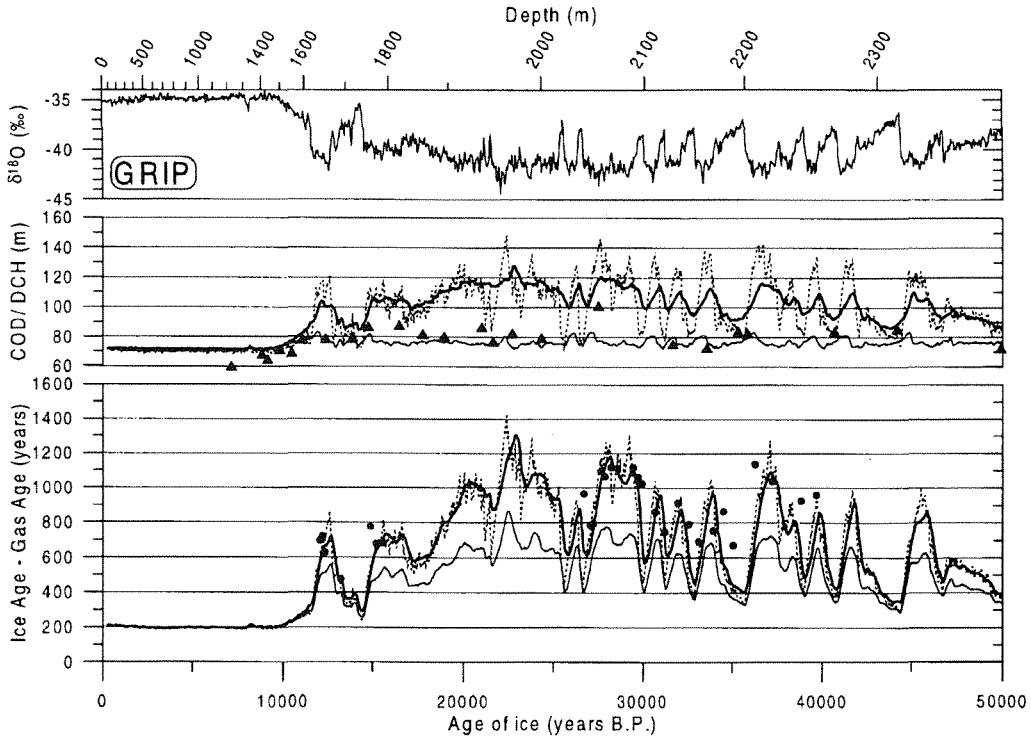

Figure 8: Extract from Fig. 2 from Schwander et al. [16]. The $\delta^{18}O$ record, model results for close-off depths (COD) and Δage, and diffusive column heights (DCH) from $\delta^{15}N$ for the GRIP ice core for the last 50 kyr BP yr (0 years BP = 1990 AD). For COD and Δage, heavy line, light line, dotted line represent the scenarios "$\alpha_{temporal}$," "$\alpha_{spatial}$," and "$\alpha_{temporal}$ without temperature diffusion," respectively. Triangles denote DCH calculated from $\delta^{15}N$ data. Circles are Δages obtained by CH_4 - $\delta^{18}O$ matching.

and the $\delta^{18}O$ record in both the GRIP and the GISP2 ice core resemble closely. For every warm event in the glacial (Dansgaard-Oeschger event) recorded in $\delta^{18}O$ a corresponding event in the CH_4 record is seen. Similarities in the records are seen as well during the increase from the glacial to the interglacial, the Younger Dryas (YD) and around 8.2 kyr where a sharp temperature decrease occurs. The rapidity with which both properties change [24, 25], coupled with the short residence time of atmospheric CH_4, make it likely that the two properties change in concert. Confirmation of the basic assumption of a synchronism between the $\delta^{18}O$ and CH_4 signal during fast climatic change comes from $\delta^{15}N$ measurements for the YD period (see below). Further the sources for CH_4 are most probably located at low latitudes. Recently it has been shown that the monsoonal activity in low latitudes reacts strongly to Dansgaard-Oeschger events [26].

Given the assumption of a synchronous increase in atmospheric CH_4 levels and Summit temperatures, Schwander et al. [16] used the CH_4 and $\delta^{18}O$ records to estimate discrete values of Δage. In Figure 8 an abstract of the GRIP results from Schwander et al. [16] is shown. The major part of the individually fitted

data fit better to the lower temperature scenario curve. The modelled as well as the 'counted' Δage estimate from the $\delta^{18}O$ and CH_4 signals is not completely independent from the time scale used. Time scales were derived from the annual layer counting and ice flow models [23, 27]. The time scales from the GRIP and GISP2 core differ significantly. These independent chronologies give us an estimate of the Δage uncertainty from the used chronology. Since the fit is also better for the lower temperature scenario for the GISP2 Δages it can be concluded, that the uncertainty of the GRIP and GISP2 chronology is negligible in this context.

Another way to test the temperature scenarios is to compare the modelled COD with the diffusive column height derived from $\delta^{15}N$ by equation 1. This height is equal to the close-off depth reduced for the height of the convection and the non-diffusive zone (see Figure 2). Thus the close-off depth of a physically reasonable scenario should always be larger than the diffusive column length. This is not the case for the major part of the diffusive column heights for the higher temperature scenario (not shown in Figure 8). The $\alpha_{temporal}$ scenario fulfils this criteria thus also $\delta^{15}N$ supports the lower temperature scenario (see Schwander et al. [16] for details).

Severinghaus et al. [12] have investigated the $\delta^{15}N$ change at the YD in view of the thermal information recorded in the $\delta^{15}N$ signal from thermal diffusion at the GISP2 site. $\delta^{15}N$ records a temperature change in the gas record. The temperature signature in $\delta^{15}N$ penetrates the firn by the speed of gas trapping which is only slightly dependent on the gas species. Thus, changes in CH_4 and $\delta^{15}N$ reach the close-off depth roughly at the same time. Detailed $\delta^{15}N$ measurements show (Figure 9) that CH_4 and $\delta^{15}N$ change synchronously (within 30 yr) for the YD [12]. This proves that our assumption of a synchronous signal of $\delta^{18}O$ and CH_4 is valid at least for the YD but probably also for other fast temperature events in the glacial.

Since $\delta^{15}N$ records a temperature change in the gas record we can determine Δage by counting the annual layers between the temperature signal recorded in water isotopes and its corresponding $\delta^{15}N$ signal. For the YD 809±20 annual layers are counted between the $\delta^{18}O$ and the $\delta^{15}N$ in the GISP2 core [12], in agreement with the deeper borehole temperature scenario. This is the same result as from the $\delta^{18}O$ and CH_4 synchronisation which is not surprising since the $\delta^{15}N$ confirms the assumption of the two signals being synchronous.

In order to use equation 2 to calculate a temperature change the thermal $\delta^{15}N$ fraction has to be extracted from the $\delta^{15}N$ signal by subtracting the fraction caused by gravitational fractionation. This fraction is not constant in time since the COD is also varying when temperature changes. The portion of gravitational and thermal fractionation can be quantified by adding the information of another isotope ratio. Severinghaus et al. [12] used Argon isotopes to show that not the entire $\delta^{15}N$ change over the YD can be associated to temperature but part results also from the change of the close-off depth. They guess that the abrupt YD-Preboreal temperature increase is 5–10 °C. This is significantly less than the temperature obtained by the Δage approach since it considers only the steep temperature increase at the end of the YD over several decades while the Δage approach includes the gradual increase after the abrupt warming. The difference

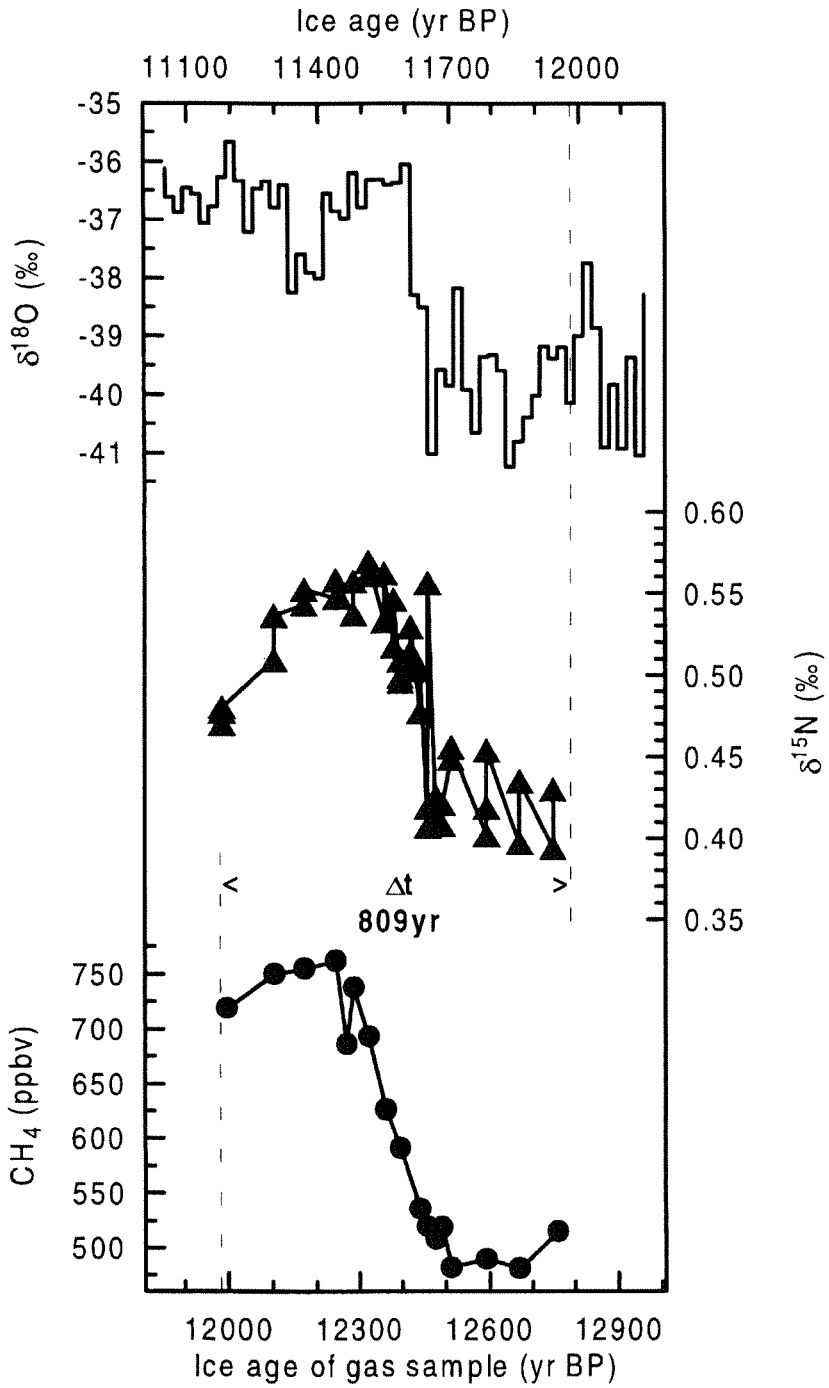

Figure 9: $\delta^{18}O$, $\delta^{15}N$ and CH_4 results for the YD period in the GISP2 core [12]. The gas records $\delta^{15}N$ and CH_4 are plotted on the ice time scale (lower X-axis) which was shifted relative to the ice time scale applying to the $\delta^{18}O$ record (upper X-axis) by 809 yr. This in order to synchronise the $\delta^{18}O$ and the $\delta^{15}N$ signal from thermal diffusion which is directly related to the temperature change recorded in $\delta^{18}O$. The shift of the two time scales is therefore an independent measure of Δage.

therefore results from the different time spans considered and is no contradiction.

7. Summary

Many processes are involved in the mixing of air in the firn. For simple conditions (no meltlayers) we can however make statements about the importance of the processes involved. Phenomenologically the firn zone can be divided into three zones: A convective zone, a diffusive zone and a non-diffusive zone (from top to bottom). The non-diffusive zone is relatively small and is located within the firn-ice transition.

The mass transport in the convective zone is dominated by convection induced by atmospheric or wind generated pressure changes. The extent of the convective zone depends strongly on the firn surface topography, the wind speed and the wind direction. However so far no quantification of the extent of the convective zone from site parameters was possible.

At flat polar sites as for instance Summit, Central Greenland molecular diffusion is the most important process that controls the mixing of gas species. Proof for the dominance of molecular diffusion comes from the close fit between measured and modelled trace gas concentrations using a pure molecular diffusion approach. The age of the gas at close-off is in the range of a decade but the atmospheric signal is recorded dispersed due to the mixing in the firn. At low accumulation sites the age distribution is additionally broadened since the time to cross the bubble formation zone is long compared to the diffusion time and the gradual close-off becomes the dominant term in the age distribution.

With a dynamical densification/heat transfer model in combination with information from the diffusion model about bubble close-off and the age of the air at close-off it is possible to calculate Δage and close-off depth under changing climatic conditions from temperature and accumulation records. This allows to establish a reliable time scale for the gas archive.

Inversely it is possible to extract the surface temperature information recorded by the trapping process through the temperature dependence of Δage. For Summit independent Δages obtained by matching of corresponding events in the methane and the $\delta^{18}O$ record were compared to calculated Δages for two temperature scenarios. Δage as well as diffusive column heights from $\delta^{15}N$, support the temperature-$\delta^{18}O$ relation based on borehole temperature profiles recently published for the GRIP and the GISP2 sites, at least for the last 40 kyr.

The $\delta^{15}N$ signal from thermal diffusion allows also to determine the surface temperature over periods of rapid temperature change. Results for the YD period for Summit are in agreement with the previous results and confirm the basic assumption of synchrony between CH_4 and $\delta^{18}O$.

Processes in the firn can be regarded as a nuisance as they complicate the interpretation of gas records. Yet the processes add additional climatic information to the trace gas and isotopic records. To extract this information a fundamental understanding of the processes and a good model approach is necessary. The understanding of processes in the firn is one aim of the ongoing European FIRETRACC/100 project.

Acknowledgements

This work was supported by the University of Bern, the Swiss National Science Foundation, and the European program ENV4-CT97-0406 "Firn Record of Trace Gases Relevant to Atmospheric Chemical Change over 100 Years" (FIRETRACC/100) grant BBW 97.0420. We would like to thank Jeff Severinghaus for providing us with his data.

References

1. Schwander, J. and Stauffer, B. *Nature* 311, 45-47 (1984).
2. Herron, M.M. and Langway, C.C., Jr. *J. Glaciol.* 25, 373-385 (1980).
3. Barnola, J.-M., Pimienta, P., Raynaud, D. and Korotkevich, Y.S. *Tellus* 43, 83-90 (1991).
4. Schwander, J., et al. *J. Geophys. Res.* 98, 2831-2838 (1993).
5. Sowers, T., Bender, M., Raynaud, D. and Korotkevich, Y.S. *J. Geophys. Res.* 97, 15683-15697 (1992).
6. Schwander, J. in *The Environmental Record in Glaciers and Ice Sheets* (eds. Oeschger, H. & Langway Jr., C.C.) 53-67 (John Wiley, New York, 1989).
7. Craig, H., Horibe, Y. and Sowers, T. *Science* 242, 1675-1678 (1988).
8. Bender, M.L., Sowers, T., Barnola, J.-M. and Chappellaz, *J. Geophys. Res. Lett.* 21, 189-192 (1994).
9. Martinerie, P., Raynaud, D., Etheridge, D.M., Barnola, J.-M. and Mazaudier, D. *Earth and Planet. Sci. Lett.* 112, 1-13 (1992).
10. Colbeck, S.C. *J. Glaciol.* 35, 209-213 (1989).
11. Sturm, M. and Johnson, J.B. *J. Geophys. Res.* 96, 11657-11671 (1991).
12. Severinghaus, J.P., Sowers, T., Brook, E.J., Alley, R.B. and Bender, M.L. *Nature* 391, 141-146 (1998).
13. Severinghaus, J.P., Bender, M.L., Keeling, R.F. and Broecker, W.S. *Geochim. Cosmochim. Acta* 60, 1005-1018 (1996).
14. Schwander, J., Stauffer, B. and Sigg, A. *Ann. Glaciol.* 10, 141-145 (1988).
15. Pimienta, P. 163 (*Univ. Sci., Tech. et Méd. de Grenoble*, Grenoble, France, 1987).
16. Schwander, J., et al. *J. Geophys. Res.* 102, 19483-19494 (1997).
17. Martinerie, P., et al. *J. Geophys. Res.* 99, 10565-10576 (1994).
18. Raynaud, D., Chappellaz, J., Ritz, C. and Martinerie, P. *J. Geophys. Res.* 102, 26607-26614 (1997).
19. Andrussov, L. in *Landolt-Börnstein. Zahlenwerte und Funktionen aus Physik, Chemie, Astronomie, Geophysik, Technik* (ed. Schäfer, K.) 516-565 (Springer-Verlag, Berlin, 1969).
20. Dansgaard, W. *Tellus* 16, 436-468 (1964).
21. Johnsen, S.J., Dansgaard, W. and White, J.W.C. *Tellus*, Ser. B 41, 452-468 (1989).
22. Cuffey, K.M., et al. *Science* 270, 455-458 (1995).
23. Johnsen, S., Dahl-Jensen, D., Dansgaard, W. and Gundestrup, N. *Tellus* 47B, 624-629 (1995).
24. Chappellaz, J., et al. *Nature* 366, 443-445 (1993).
25. Brook, E.J., Sowers, T. and Orchardo, J. *Science* 273, 1087-1091 (1996).
26. Schulz, H., von Rad, S. and Erlenkeuser, H. *Nature* 393, 54-57 (1998).
27. Alley, R.B., et al. *Nature* 362, 527-529 (1993).

28. Schwander, J. in *Chemical Exchange Between the Atmosphere and Polar Snow* (eds. Wolff, E.W. & Bales, R.C.) 527-540 (1996).